

3. Results

3.1 Histology and scanning electron microscopy (SEM) of the adipose eyelid

The paraffin sections of the adipose eyelid with H&E staining showed that there were three layers of adipose eyelid from the outer toward the inner side (Figure 1).

The adipose eyelid was like a sandwich: its outer and inner layers were both the epithelial tissue, and the middle, the thickest layer, was the connective tissue but not adipose tissue, because of the positive reaction in the Pico-Ponceau with Hematoxylin staining (Figure 2) and the negative reaction in the Oil Red O staining (Figure 3).

Compared with the artery section, the negative reaction of adipose eyelid section in Orcein staining indicated that this connective tissue did not have elastic fibers (Figure 4), but might contain either collagen fibers or reticular fibers. The outer layer of epithelial tissue was multiple cells and the inner layer was the single cellular layer. In the histological sections with H&E staining, the inner single layer epithelium tissue was not as clear as the outer multiple layer epithelium tissue, but it presented typical epithelial cell under SEM. The SEM also showed that the outer layer was covered by mucous (Figure 5).

3.2 Histochemistry of adipose eyelids

A series of different staining methods were used to identify the compositions of

adipose eyelids. In PAS staining, the positive reaction of adipose eyelid showed pink coloration which implied that it was of carbohydrate nature (Figure 6). The adipose eyelid in alcian blue, pH 2.8 staining displayed blue green color which meant it was acid mucopolysaccharides substance (Figure 7). Because the section of Alcian Blue, pH 2.8 staining was fixed in the solution of formalin: 100% alcohol = 1: 9, the fast dehydration made the outer multiple layers epithelial tissue part separated easily from the medial connective tissue part and the nuclei showed red color. The Alcian Blue, pH 1.0 staining method was employed to differentiate two forms of mucopolysaccharides, sulfated or nonsulfated mucosubstances. The adipose eyelid in this staining exhibited greenish blue color and the results pointed out that it was sulfated mucosubstances (Figure 8). The Aldyhyde Fuchsin-Alcian Blue staining method was used to differentiate two forms of sulfated mucosubstances: connective tissue mucopolysaccharides (strongly sulfated) and epithelial sulfomucins or epithelial mucosubstances (weekly sulfated). The purple color in the Aldyhyde Fuchsin-Alcian Blue staining section (Figure 9) and the positive reaction in the PAS staining revealed that the substance of adipose eyelid was either the epithelial sulfomucins or epithelial mucosubstances (Sheehan 1980).

3.3 Collagen extraction and peptide mapping

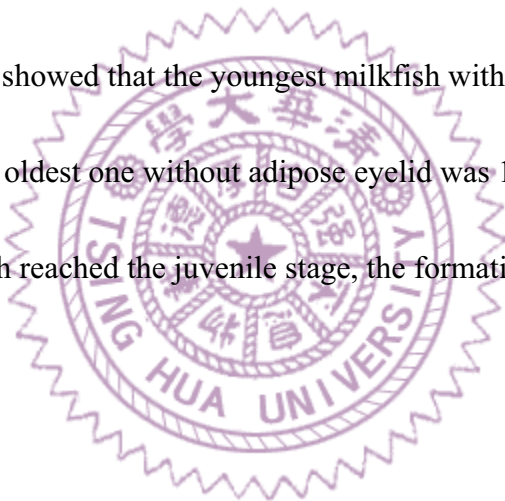
A total of about 0.2 g collagens were extracted from a 7 g of adipose eyelids, the

yield of collagen was about 2.86 %. After lyophilization, the dry collagens looked like regular cottons (Figure 10). Collagen was the trimer structure, and it was combined by 3 α chains. These three α chains could be homopeptide or heteropeptide. In the SDS-PAGE gel, collagen which was extracted from adipose eyelids and the calf skin type I collagen both showed the $\alpha 1$ and $\alpha 2$ chains around 116 KDa, and the concentration of $\alpha 1$ chain was twice as much as that of $\alpha 2$ chain (Figure 11). This indicated that the collagen extracted from the adipose eyelids was the type I collagen which had two $\alpha 1$ chains and one $\alpha 2$ chain. The molecular weight of $\alpha 1$ chain of the adipose eyelid type I collagen was slightly heavier than that of the calf skin type I collagen, this might due to the difference of amino acid compositions of type I collagen $\alpha 1$ chain between the calf skin and the milkfish adipose eyelid. Because the collagen had the intra- and inter- molecular cross-link, it was hard to be denatured. Besides the noncross-linked monomers, $\alpha 1$ chain and one $\alpha 2$ chain; the dimer (β) or trimer (γ) form both could be observed in SDS-PAGE gel (Figure 11).

3.4 The ontogenetic development of the adipose eyelid

Both the histological sections and dissection microscope observation showed that the adipose eyelid was absent in the larval milkfish head, but was present in the juvenile's (Figures 12, 13). The ontogenetic development of adipose eyelid began at the circumambieny of the eye socket, and then gradually expanded to the center of

the eyeball. Finally, the extending adipose eyelid would coalesce and a chamber between the eyelid and eye was formed. Because the peripheral adipose eyelid formed earlier than the center part, the central part of the adipose eyelid was the part of the whole adipose eyelid. The H&E staining sections also showed that the medial connective tissue part did not occupy the most portions at the beginning of the formation of the adipose eyelid, but it continued to grow and the thickening of the adipose eyelid was mainly on this part. The standard length of milkfish with or without adipose eyelid showed that the youngest milkfish with adipose eyelid was 10.5 mm in SL and the oldest one without adipose eyelid was 18.7 mm in SL (Figure 14). Before the milkfish reached the juvenile stage, the formation of adipose eyelid was completed.



3.5 Histology of retina

The retina of the milkfish could be divided into six layers (Figure 15): (1) the rods and cones layer which contained the outer segments of the rod cells and cone cells; (2) the outer nuclear layer (ONL) which contained the nuclei of the rods and cones, and the positions of the cone nuclei were usually higher than those of the rods; (3) the outer plexiform layer (OPL) which contained the synapses of the photoreceptor cells' dendrites and the axons of the bipolar cells and horizontal cells; (4) the inner nuclear layer (INL) which contained the nuclei of the bipolar, horizontal,

amacrine, and neuroglial Müller's cells; (5) the inner nuclear layer (INL) which contained the axons of the bipolar cells synapse with the dendrites of the amacrine and ganglion cells; (6) In the ganglion cell layer (GCL), the cell bodies of the ganglion and neuroglial cells were found (Figure 15). Because the processing from visual cells to the ganglion cells was convergence, the nuclei of the ONL, INL, and GCL became less and less. The paraffin radial sections with H&E staining revealed that the milkfish retina was a duplex retina, but there was only one type of cone cell, i.e. single cone, in the milkfish retina. The double cone or the twin cone cells were absent from the milkfish retina. The resin tangential sections stained with Toluidine Blue O also showed that the single cone cell did not arrange in a regular order. The paraffin sections of light-adapted and dark-adapted retina revealed the movement of the screening pigments inside the visual cell. In the light-adapted eyes, the pigment invaded into the rods and cones layer and the rods were higher than cones; in the dark-adapted eyes, the pigment retreated and the cones moved to the outer part of the rods and cones layer (Figure 16).

3.6 Plasma and adipose eyelid fluid analyses

The osmolarities of the chamber fluid varied when the milkfish was transferred acutely to different salinity media. Compared with the plasma osmolarities which was maintained around 300 to 420 mmol/Kg, the variations of the chamber fluid

osmolarities were much higher than those of plasma when milkfish was transferred from seawater to freshwater and vice versa. Interestingly, the chamber fluid osmolarities were always higher than those of the ambient waters. In the freshwater condition, the osmolarity of the chamber fluid was about 350 mmol/Kg which was slightly higher than the plasma osmolarity but without statistical significance ($P>0.05$).

When the milkfish adapted to the seawater salinity, the osmolality of the chamber fluid was statistically significantly higher than those of the seawater and plasma osmolalities. It took one to two days for the chamber fluid osmolality to reach to a new equilibrium with the new ambient salinity (Figure 17). The chloride concentrations of the chamber fluid and the plasma were not statistically different ($P>0.05$) in the long-term freshwater adaptation, but it was statistically higher ($P<0.05$) than those of the plasma and the environment in the long-term seawater adaptation.

When milkfish was transferred to a new salinity condition, it took one day at most to adjust to the new chloride concentration (Figures 18, 19). The change of potassium concentrations was similar to that of the chloride concentrations. In the long-term freshwater adaptation, there was no statistical difference ($P>0.05$) in terms of potassium concentration between the chamber fluid and plasma. Yet in the long-term seawater adaptation, the potassium concentrations of the chamber fluid had the statistically higher values than those of the plasma and the environment. The potassium concentration also took one day at most to reach to the new equilibrium

(Figures 20, 21). The sodium concentration was statistically higher ($P < 0.05$) than those of the plasma and the surroundings whether in the long-term seawater or freshwater adaptation. During the transfer, the sodium concentration took less than one day to reach to the new equilibrium (Figures 22, 23). The proteins were also present in the chamber fluid, but the concentrations of them in the long-term freshwater and long-term seawater adaptation were not statistically different ($P > 0.05$) from each other (Figure 24).

3.7 Immunostaining and Western blotting

The cryosections of the long-term seawater and freshwater adapted adipose eyelid were immunostained with $\alpha 5$ and T4 antibodies and it revealed that the NKA and NKCC were both presented in the outer multiple layers epithelium tissue (Figures 25, 26). The confocal micrographs also revealed that the NKA was expressed in the baselateral membrane of the epithelium cell of the outer multiple layers epithelium tissue in both long-term seawater and freshwater adapted conditions (Figures 27). The $\alpha 5$ antibody was designed to conjugate the α subunit of the NKA protein whose molecular weight was about 112 KDa. In the Western blotting of NKA, the proteins extracted from the long-term seawater and freshwater adapted specimens also expressed the reactive band at the appropriate site (Figure 28). The molecular weight of the NKCC protein was about 145-205 KDa. But in the Western blotting of NKCC,

the reactive protein was only about 50 KDa, and the expression of this protein became less and less after the milkfish was transferred from freshwater to seawater (Figure 29). Without the proper molecular weight data as an indicator, it was hard to decide if the T4 conjugated protein was the NKCC.

3.8 Spectral transmission of adipose eyelid, cornea, and lens

The data from USB-2000 spectrophotometer showed that the adipose eyelid filtered out light of wavelength shorter than 305 nm, and the lens filtered light with wavelength shorter than 319 nm. The transmission spectrum of the cornea was quite unlike the ones of adipose eyelid and lens. It blocked out light wavelength shorter than 337 nm. The T50 value of the adipose eyelid was about 323 nm, and it was 386 nm and 359 nm for the cornea and lens, respectively (Figure 30).

3.9 Refractive state of the juvenile milkfish

The photoretinoscope pictures revealed that the eyes of milkfish were hyperopic (Figure 31), and the diopter was 5.03 ± 0.26 . After the adipose eyelid was removed, the diopter was 4.18 ± 0.66 (Figure 32). In terms of diopter values, there was no statistical difference ($P > 0.05$) between the milkfish eye with adipose eyelid and the one without adipose eyelid. These data indicated that the adipose eyelid didn't work as a lens to help eye focusing.

3.10 Visual spectra of the larval and the juvenile milkfish

The MSP measurements indicated that the larval milkfish had four types of single cone cells in the retina. They were the red cone, the green cone, the blue cone, and the violet cone cells. The maximal absorbance wavelength (λ_{\max}) for the red cone cells were 578.61 ± 10.39 nm, for the green cone cells were 506.56 ± 10.24 nm, for the blue cone cells were 468.45 ± 9.78 nm, for the violet cone cells were 423.16 ± 9.12 nm, and for the rod cells were 507.37 ± 5.30 nm (Figure 33). The juvenile milkfish which had the red cone cells ($\lambda_{\max} = 580.27 \pm 6.05$ nm), the green cone cells ($\lambda_{\max} = 502.28 \pm 8.48$ nm), the blue cone cells ($\lambda_{\max} = 441.97 \pm 7.70$ nm), and the rod cells ($\lambda_{\max} = 497.05 \pm 7.81$ nm) (Figure 34). No violet cone cells could be found and the blue cone cell had the statistically significant spectral shift to shorter wavelength for about 30 nm ($P < 0.05$) when the milkfish grew from larval into the juvenile stage.